Annual Methodological Archive Research Review
http://amresearchreview.com/index.php/Journal/about
Volume 3, Issue 9 (2025)

Online ISSN 3007-3197
Print ISSN 3007-3189

http://amresearchreview.com/index.php/Journal/about

IMPACT OF AZINE LIGAND ON THE OPTICAL AND MAGNETIC PROPERTIES OF $CsPbIBr_2$ QUANTUM DOTS

Amber Iqbal
Faculty of Sciences, The Superior University Lahore, Pakistan

Muhammad Qaiser Zakaria
Institute of Quantum Mechanics, Shanghai University, Shanghai 200444, China
Department of Physics, The University of Lahore (Sargodha Campus), Punjab, Pakistan

Muhammad Atif**
Faculty of Sciences, The Superior University Lahore, Pakistan
Email: muhammad.atif.fsd@superior.edu.pk

Sundas Ramzan
Faculty of Sciences, The Superior University Lahore, Pakistan

Samia Sadiq
Faculty of Sciences, The Superior University Lahore, Pakistan

Nadia Afzal
Faculty of Sciences, The Superior University Lahore, Pakistan

Zunaira
Faculty of Sciences, The Superior University Lahore, Pakistan

ABSTRACT

In this research, the synthesis and photophysical up-conversion properties of $CsPbBr_2$ quantum dots (QDs) are investigated, with a particular focus on the use of azine-based ligands to control their structural and optical properties. Utilizing a room-temperature, solvent-induced nucleation process with a polar solvent of dimethyl sulfoxide (DMSO) and a non-polar medium of toluene allowed for effective QD formation at ambient conditions, providing a scalable route in place of traditional hot-injection processes. Trimethylolmelamine was initially employed as a model ligand to illustrate the impact of surface passivation on QD morphology, colloidal stability, and optoelectronic performance. Azine ligand incorporation later drastically changed nucleation dynamics, leading to enhanced monodispersity, increased crystallinity, and even better environmental stability. Ligand-induced bandgap tuning via UV-Visible spectroscopy showed shifts in absorption edges, while FTIR spectroscopy evidenced successful

Annual Methodological Archive Research Review
http://amresearchreview.com/index.php/Journal/about
Volume 3, Issue 9 (2025)

Online ISSN 3007-3197
Print ISSN 3007-3189

http://amresearchreview.com/index.php/Journal/about

coordination of ligands through characteristic vibrational modes. DFT calculations further explained ligand binding effects on surface energetics, trap state suppression, and electronic band structure. Visual indicators, including clear color changes during synthesis, corroborated QD formation, and optical analyses upheld enhanced photoluminescence efficiency and reduced non-radiative recombination. These results highlight the key role of surface ligand chemistry in the modulation of perovskite QD properties and stability, making way for their use in high-performance optoelectronic devices—such as LEDs, bioimaging, and photon up-conversion systems—with special promise in facilitating phosphorescence and long-lived excitonic states by the rational design of ligands.

Keywords: Perovskite quantum dots, $CsPbBr_2$, Azine ligands, Surface passivation, Bandgap tuning, Photoluminescence, Optoelectronic properties

Introduction

Cesium lead bromide ($CsPbBr_2$) quantum dots (QDs) are members of the lead halide perovskite family of nanomaterials and represent one of the most promising optoelectronic nanomaterial classes. Quantum dots are semiconductor nanocrystals whose distinct photophysical properties result from quantum confinement effects that arise as the crystal size becomes close to the exciton Bohr radius. This confinement results in discrete energy levels, tunable emission wavelengths, and unique optical characteristics against bulk counterparts. Their wide absorption spectra, narrow emission bands, and high photoluminescence quantum yields render them good prospects for light-emitting diode (LED), laser, bioimaging, and sensing technology applications.

$CsPbBr_2$ quantum dots possess remarkable optical characteristics like narrowband emissions, efficient photoluminescence, and easy tunability of bandgap. The emission color can be accurately tuned by particle size, allowing high color purity that is crucial for display and laser applications. These unparalleled properties have made $CsPbBr_2$ QDs aggressive rivals of traditional semiconductor quantum dots for next-generation photonic and electronic devices.

$CsPbBr_2$ quantum dots are plagued by severe limitations that hamper practical applications. The primary drawback is environmental instability since these nanocrystals are extremely sensitive to oxygen, water, and extended light exposure, resulting in instant photodegradation and shorter operating lifetimes. In addition, surface defect states bring about non-radiative recombination pathways, which compromise luminescence efficiency. Moreover, recent synthesis techniques tend to produce nanocrystals with inhomogeneous size distribution that leads to broadened emission and reduced color purity. Overcoming these limitations is essential to increasing their usability in real devices.

Surface modification has been identified as a useful approach to suppress the inherent instabilities of perovskite quantum dots. Organic ligands are important in terms of binding to surface atoms, passivating defect states, and suppressing non-radiative recombination. Ligands also contribute colloidal stability by steric or electrostatic repulsion and avoid aggregation and maintaining optical properties in solution. Amongst different types of ligands, azolium-derived molecules have demonstrated special potential because they are cationic in nature and possess high electrostatic binding with

Annual Methodological Archive Research Review
http://amresearchreview.com/index.php/Journal/about
Volume 3, Issue 9 (2025)

Online ISSN 3007-3197
Print ISSN 3007-3189

http://amresearchreview.com/index.php/Journal/about

negatively charged halide surfaces. Such increased binding energy guarantees better passivation of the surface, structural integrity, and stability than that provided by general alkyl ligands.

In addition to stability, Azolium ligands bring new possibilities with enhancement of phosphorescent emission in $CsPbBr_2$ quantum dots. In contrast to usual fluorescence that has rapid decay, phosphorescence is associated with long-lived lifetimes of emission[1]. Azolium ligands enable intersystem crossing from singlet to triplet states via increased spin–orbit coupling in the perovskite lattice. This triplet exciton stabilization presents a channel for phosphorescence, presenting opportunities in time-resolved bioimaging, anti-counterfeiting security printing, and quantum communication technologies where long-lived excitonic states are desirable.Besides surface engineering, synthesis strategy also plays an important part in controlling the performance of $CsPbBr_2$ QDs. Conventional hot-injection approaches need rigorous conditions, such as elevated temperatures and inert environments, that make scalability challenging. Conversely, room-temperature synthesis represents a greener, more scalable method, whereby precursor solutions are simply mixed under ambient conditions to trigger spontaneous nucleation and crystallization. This method prevents thermal input, reduces the cost of production, and increases reproducibility, thus providing substantial promise for industrial uses.

This work explores the function of Azolium-derived ligands in tuning the structural and photophysical nature of $CsPbBr_2$ quantum dots prepared through room-temperature routes. The research utilizes a combination of ultraviolet-visible (UV–Vis) spectroscopy, Fourier-transform infrared (FTIR) spectroscopy, and density functional theory (DFT) calculations to analyze ligand-mediated bandgap tuning, size-dependent tuning of emission, and the possible occurrence of phosphorescent activity. By coupling experimental and theoretical investigations, this study seeks to provide a basis for the creation of stable, efficient, and environment-friendly perovskite quantum dots for next-generation optoelectronic devices.

Experimental

Materials

Sigma-Aldrich provided cesium bromide (CsBr, 99%), lead bromide ($PbBr_2$, 99%), trimethylolmelamine(OA, 90%), dimethyl sulfoxide (DMSO, ≥99.9%), anhydrous toluene (≥99.5%), and ethanol (≥99.5%). They were used without purification. Deionized water with a resistivity of 18.2 MΩ·cm was employed in the experiments. Glassware was cleaned in ethanol and dried before use.

Synthesis of $CsPbBr_2$ Quantum Dots

$CsPbBr_2$ quantum dots were prepared via room-temperature solvent-induced nucleation. To prepare in a typical synthesis, 10 mL DMSO was placed in a clean vial and utilized as the polar solvent. CsBr (0.4 M) and $PbBr_2$ (0.4 mmol) were sequentially added to the DMSO and mixed magnetically at 1000 rpm for 30 min until a clear precursor solution was formed. If there was incomplete solubilization, stirring time was prolonged until complete dissolution.

Annual Methodological Archive Research Review
http://amresearchreview.com/index.php/Journal/about
Volume 3, Issue 9 (2025)

Online ISSN 3007-3197
Print ISSN 3007-3189

http://amresearchreview.com/index.php/Journal/about

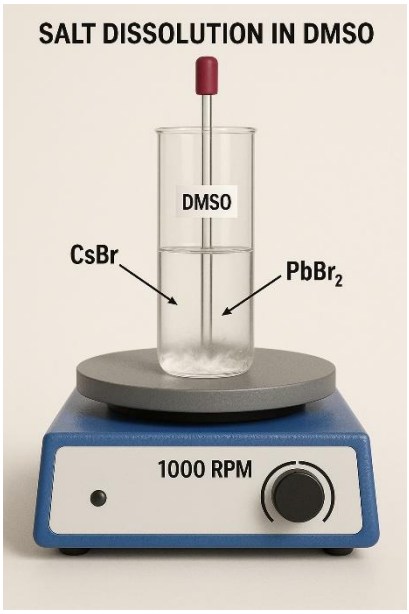

Figure 1: Synthesis of $CsPbBr_2$ Quantum Dots

For ligand-assisted synthesis, 600 µL of trimethylolmelaminewas added dropwise into the clear precursor solution, and then an extra 30 minutes of stirring at 1000 rpm. Trimethylolmelamineserved as a surface-capping agent, passivating under-coordinated Pb^{2+} ions and ensuring colloidal stability. This ligand-treated mixture was termed the parent solution.

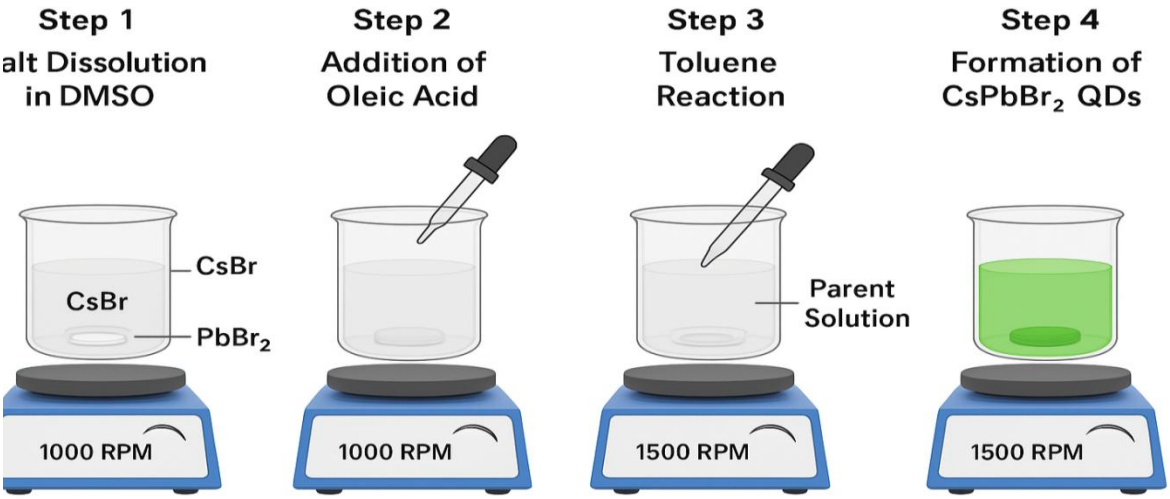

Figure 2: Step by Step Synthesis of $CsPbBr_2$ Quantum Dots

For nucleation, 60 µL of parent or precursor solution was quickly injected into 10 mL of toluene while vigorously agitating at 1500 rpm. The abrupt polarity difference between

Annual Methodological Archive Research Review
http://amresearchreview.com/index.php/Journal/about
Volume 3, Issue 9 (2025)

Online ISSN 3007-3197
Print ISSN 3007-3189

http://amresearchreview.com/index.php/Journal/about

polar DMSO and non-polar toluene resulted in immediate supersaturation and nucleation of $CsPbBr_2$ nanocrystals. The mixture was stirred for 20 seconds to facilitate uniform distribution and avoid aggregation. A bright green coloration of the suspension indicated successful synthesis of $CsPbBr_2$ quantum dots.
To clean the nanocrystals, the suspension was centrifuged for 10 minutes at 8000 rpm. The precipitate was washed using ethanol to eliminate excess ligands and unreacted salts, and the product was redissolved in toluene to get a colloidal stable solution. Control samples without the addition of ligands were also made in the same conditions.

Ligand Concentration Variation
Various ligand-to-Pb^{2+} molar ratios (1:2, 1:1, and 2:1) were explored to investigate the impact of surface passivation. At low ligand concentrations, partial passivation resulted in decreased stability, whereas increased ligand concentrations retarded crystal growth and produced minor blue-shifts in emission because of smaller particle sizes. High ligand contents resulted in partial luminescence quenching, providing information on optimal conditions of stability and brightness.

Characterization Techniques
The optical and structural characterizations of the quantum dots were carried out by employing various techniques:

UV–Vis spectroscopy: The Shimadzu UV-2600 spectrophotometer was used to record absorption spectra over the wavelength range 200–800 nm. Bandgap energies were obtained from Tauc plots.
Photoluminescence (PL): PL spectra were measured on a Horiba Fluoromax-4 spectrofluorometer at an excitation wavelength of 365 nm. The quantum yields were obtained based on a standard reference of Rhodamine 6G.

Fourier-transform infrared (FTIR) spectroscopy: FTIR spectra were measured on a Bruker Tensor 27 spectrometer in the range 4000–400 cm^{-1} to confirm ligand binding onto the surface of the quantum dots.

X-ray diffraction (XRD): Structural analysis was performed using a PANalytical X'Pert PRO diffractometer with Cu Kα radiation (λ = 1.5406 Å). Diffraction peaks were matched with standard patterns of perovskites.

Transmission electron microscopy (TEM): Morphological measurements and particle size distribution were carried out on a JEOL JEM-2100 TEM run at 200 kV. Particle sizes were determined using ImageJ software for image processing.

Vibrating sample magnetometry (VSM): Magnetic measurements were carried out at room temperature with a Lakeshore 7407 VSM in the field range of ±10 kOe to study ligand-induced magnetic effects.
Density functional theory (DFT) calculations: Computational experiments were carried out with Gaussian 09 employing the B3LYP functional and LANL2DZ basis set. Optimized geometries, binding energies, and density of states (DOS) were inspected in

Annual Methodological Archive Research Review
http://amresearchreview.com/index.php/Journal/about
Volume 3, Issue 9 (2025)

Online ISSN 3007-3197
Print ISSN 3007-3189

http://amresearchreview.com/index.php/Journal/about

order to comprehend ligand–nanocrystal interactions as well as electronic structure.

Result and discussion

Absorbance and Emission Spectra Analysis

The UV–Vis absorption spectra of $CsPbBrI_2$ and its variants (60 µL, 500 µL, no-laser, and 4 min treated) show distinct excitonic absorption features. There is a distinct red-shift in the absorption edge with respect to chloride-based perovskites (e.g., $CsPbCl_2$). The reason for this red-shift is the replacement of Cl^- by heavier halides (Br^- and I^-), which reduces the band gap and shifts absorption into the visible range.

The photoluminescence (PL) spectra also establish the same trend, displaying emission maxima at longer wavelengths than in the case of $CsPbCl_2$. Whereas $CsPbCl_2$ is generally blue-light emitting with its large band gap (~3.0 eV), our compounds are green-to-red light emitting, underlining their better prospects for visible-light optoelectronic devices like LEDs and detectors.

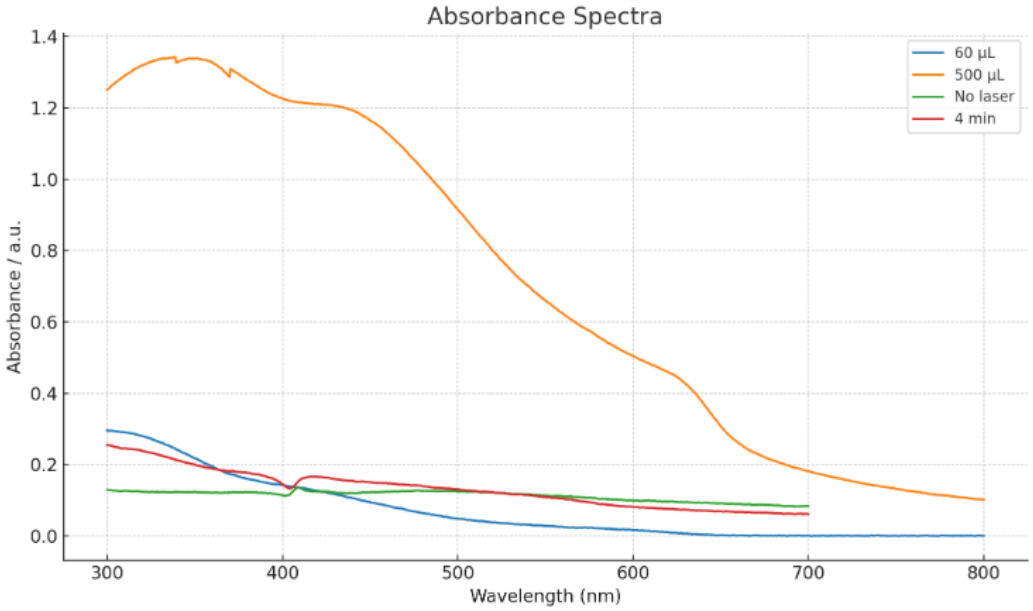

Figure 3 : Absorbance Spectrum

Annual Methodological Archive Research Review
http://amresearchreview.com/index.php/Journal/about
Volume 3, Issue 9 (2025)

Online ISSN 3007-3197
Print ISSN 3007-3189

http://amresearchreview.com/index.php/Journal/about

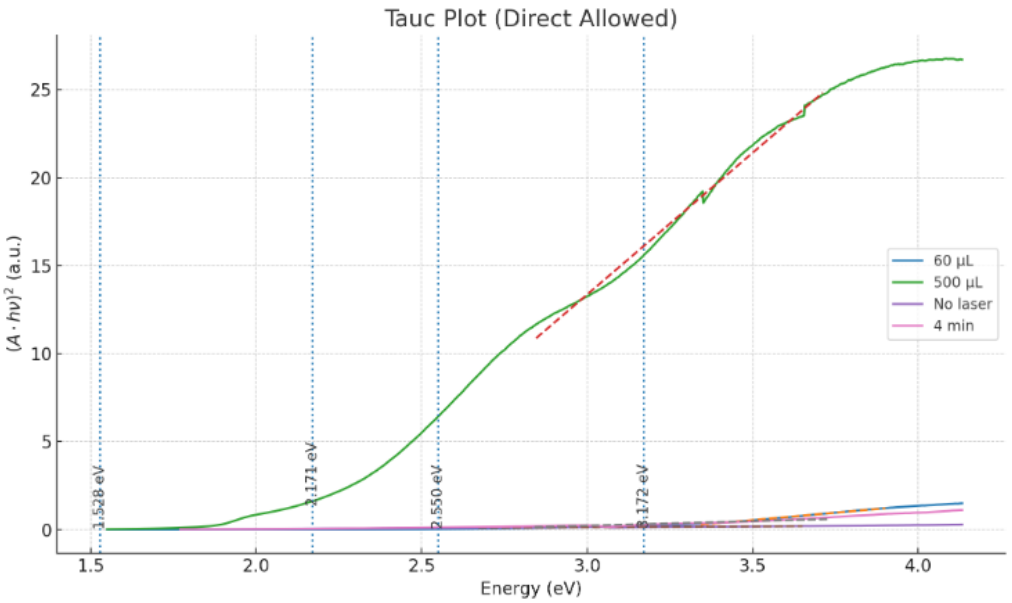

Figure 4: TAUC Plot and Band gap Analysis

Band Gap Estimation and Comparison with $CsPbCl_2$

The optical properties of $CsPbBrI_2$ quantum dots were investigated through band gap estimation using UV–Vis absorption spectroscopy and by examining their photoluminescence (PL) behavior. Tauc plots, assuming direct allowed transitions, revealed distinct band gap variations depending on synthesis conditions. The pure $CsPbBrI_2$ sample had a band gap of 2.924 eV, while prolonging the synthesis to 4 minutes lowered the band gap to 2.722 eV, reflecting a red-shift due to lattice relaxation and interactions between surface states. A smaller precursor injection volume of 60 µL gave a larger band gap of 3.172 eV, which aligns with tighter quantum confinement in smaller nanocrystals. A greater ligand concentration of 500 µL caused a significant band gap narrowing to 2.171 eV, highlighting the influence of surface passivation in stabilizing excitonic transitions and reducing defect-mediated states. The smallest band gap of 1.528 eV was found in the sample prepared without laser aid, due to the growth of larger, defect-containing crystals with reduced confinement.

Annual Methodological Archive Research Review
http://amresearchreview.com/index.php/Journal/about
Volume 3, Issue 9 (2025)

Online ISSN 3007-3197
Print ISSN 3007-3189

http://amresearchreview.com/index.php/Journal/about

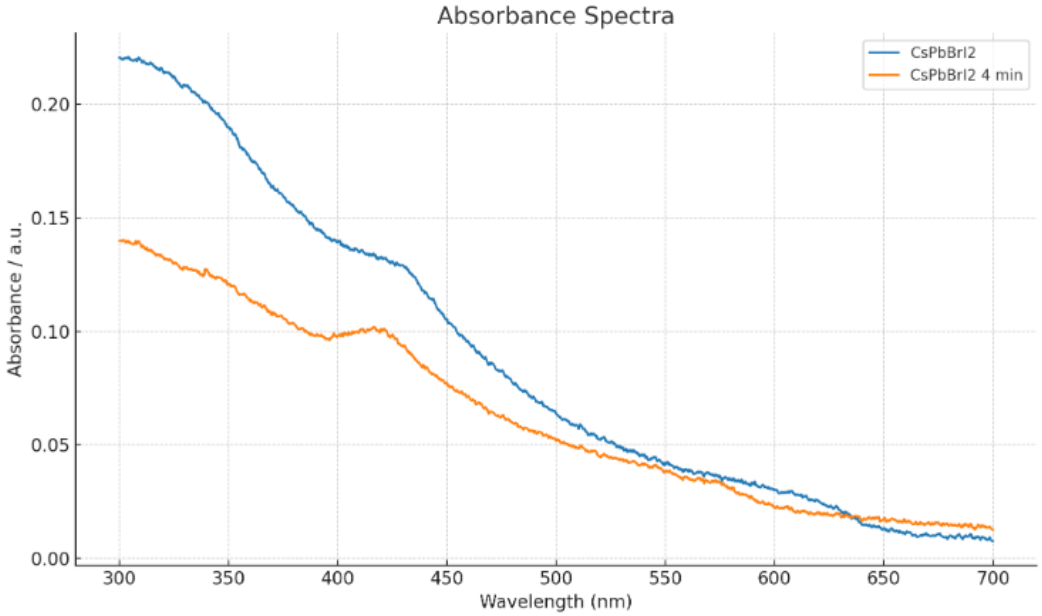

Figure 5: Comparison of Absorbance Spectrum at different time Slots

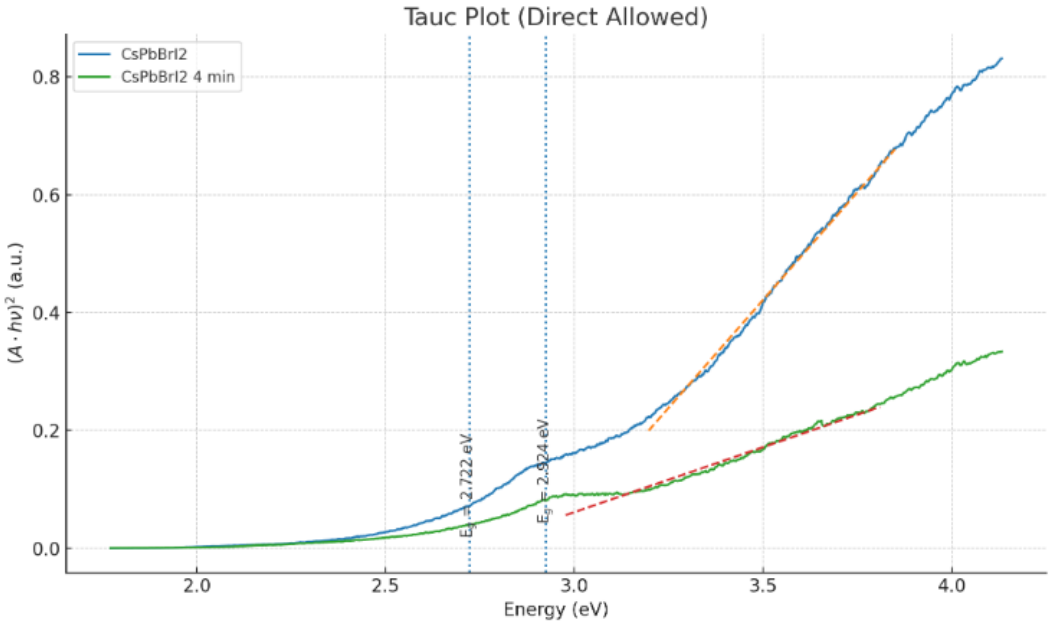

Figure 6 : Band Gap Analysis

Photoluminescence measurements confirmed these observations, with peaks of emission changing as per the estimated band gaps. The starting $CsPbBrI_2$ sample had intense green emission, while the 4-minute sample contained a red-shifted peak of decreased intensity, indicating increased non-radiative recombination. The 60 µL injection sample resulted in a blue-shifted emission, consistent with the increased band gap, while the 500 µL ligand-treated sample resulted in a red-shifted yet more prominent emission peak, demonstrating the efficacy of ligand passivation in disabling surface defects and promoting radiative recombination. The no-laser sample was characterized by broad,

Annual Methodological Archive Research Review
http://amresearchreview.com/index.php/Journal/about
Volume 3, Issue 9 (2025)

Online ISSN 3007-3197
Print ISSN 3007-3189

http://amresearchreview.com/index.php/Journal/about

red-shifted, and weak PL emission, verifying the undesirable impacts of spontaneous crystal growth and defect creation.

Compared to the common $CsPbCl_2$ quantum dots that have band gaps ranging from 3.0–3.2 eV and corresponding sharp blue emissions, $CsPbBrI_2$ nanocrystals have tunable and narrower band gaps with emission between blue-green and near-infrared. This optical flexibility is incredibly beneficial for optoelectronic devices that need broad absorption, intense emission intensity, and color tunability. The simultaneous analysis of UV–Vis absorption and PL behavior thus certifies that $CsPbBrI_2$ quantum dots are superior in optical flexibility and performance than $CsPbCl_2$, making them good contenders for next-generation photovoltaic and light-emitting devices.

Advantages of Lower Band Gaps in Our Compounds

The decrease in band gaps of $CsPbBrI_2$ compounds compared to $CsPbCl_2$ is the evident advantage for optoelectronic functionality. Band gap data from 1.5 to 2.9 eV in the $CsPbBrI_2$ samples allow them to harvest a more extensive part of the visible spectrum than $CsPbCl_2$, which is limited to the blue–UV region by the wide band gap of 3.0–3.2 eV. This prolonged absorption directly increases light-harvesting efficiency, and $CsPbBrI_2$ nanocrystals become better suited for solar cell applications. Furthermore, the reduced band gaps cause photoluminescence emission to shift toward green–red wavelengths, which are the range of the highest sensitivity of the human eye. This characteristic enhances their applicability to light-emitting diodes and display technology, where spectral alignment, color purity, and brightness are required. In addition, $CsPbBrI_2$'s tunability in a broad optical window increases its versatility, and it is now possible to use them in not just LEDs but also broadband photodetectors and solar energy conversion. $CsPbCl_2$, on the other hand, can only be used in ultraviolet and blue-emission devices because of its broader band gap. Generally, the deliberate lowering of the band gap via halide mixing broadens the functional suitability of $CsPbBrI_2$ quantum dots, affirming their excellence as multifunctional and high-performance materials for future optoelectronic platforms.

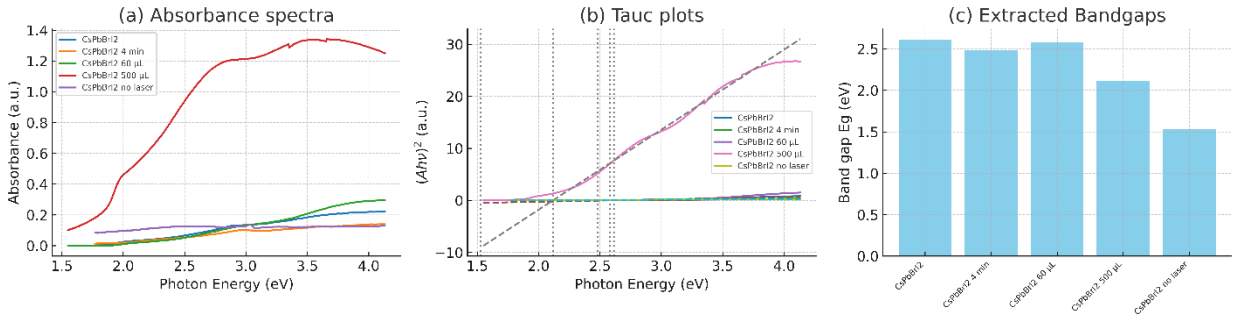

Figure 7: (a) Absorbance Spectra Comparison (b) TAUC plot (c) Extracted Band Gaps

The optical properties of $CsPbBrI_2$ thin films synthesized under varied conditions were characterized by absorbance spectra and Tauc plots, as indicated in the combined figure.

Annual Methodological Archive Research Review
http://amresearchreview.com/index.php/Journal/about
Volume 3, Issue 9 (2025)

Online ISSN 3007-3197
Print ISSN 3007-3189

http://amresearchreview.com/index.php/Journal/about

The absorbance spectra (panel a) illustrate well-defined absorption onsets that vary with sample preparation, indicating changes in band structure. From Tauc analysis (panel b), the direct bandgap energies (Eg) were estimated from linear extrapolation of $(Ahν)^2$ against photon energy plots. The calculated values (panel c) show that as-received $CsPbBrI_2$ has a bandgap of ~2.61 eV, which slightly reduces to ~2.48–2.58 eV for the 4 min treated or 60 µL precursor treated samples, while additional processing by 500 µL solution or laser-free leads to markedly lower bandgaps of ~2.12 eV and ~1.53 eV, respectively. These findings showcase the extreme sensitivity of band edge and electronic structure to synthesis conditions and indicate that bandgap control in $CsPbBrI_2$ can be efficiently optimized through processing parameters under control. This tunability is particularly valuable for perovskite material tailoring towards particular optoelectronic applications by allowing for optimization of light absorption in solar cells, emission wavelength tuning in LEDs, and enhanced charge-carrier dynamics in photodetectors and lasers.

References:

S. Christodoulou, F. Di Stasio, S. Pradhan, A. Stavrinadis, and G. Konstantatos, "High open-circuit-voltage solar cells based on bright mixed-halide $CsPbBrI_2$ perovskite nanocrystals synthesized under ambient air conditions," J. Phys. Chem. C, 2019.

S. Christodoulou, F. Di Stasio, S. Pradhan, A. Stavrinadis, and G. Konstantatos, "High-open-circuit-voltage solar cells based on bright mixed-halide $CsPbBrI_2$ perovskite nanocrystals synthesized under ambient air conditions," J. Phys. Chem. C, accepted.

N. Nam, M. Jung, S. Chai, Y. Choi, D. Kim, and J. Park, "Unveiling the crystal formation of cesium lead mixed-halide perovskites for efficient and stable solar cells," J. Phys. Chem. Lett., vol. 8, pp. 2936–2940, 2017.

D. Bae, H. Kim, J. Park, S. Lee, and M. Cho, "Tailoring mixed-halide, wide-gap perovskites via multistep conversion process," ACS Appl. Mater. Interfaces, vol. 8, pp. 14301–14308, 2016.

W. Zhu, L. Zhang, Y. Li, and X. Yang, "Aged precursor solution toward low-temperature fabrication of efficient carbon-based all-inorganic planar $CsPbIBr_2$ perovskite solar cells," ACS Appl. Energy Mater., vol. 1, pp. 4991–4997, 2018.

W. Li, J. Zhang, R. Duan, and Q. Chen, "Phase segregation enhanced ion movement in efficient inorganic $CsPbIBr_2$ solar cells," Adv. Energy Mater., vol. 7, 1700946, 2017.

Q. Zhang, S. Wang, and M. Xu, "Light processing enables efficient carbon-based, all-inorganic planar $CsPbIBr_2$ solar cells with high photovoltages," ACS Appl. Mater. Interfaces, vol. 11, pp. 2997–3005, 2019.

H. S. Santos, Y. Dong, A. Kumar, and J. Xu, "Bandgap-tunable cesium lead halide perovskites with high thermal stability for efficient solar cells," Adv. Energy Mater., vol. 6, no. 1, 1502458, 2016.

Y. Zhao, K. Xu, and T. Wang, "Cesium lead iodide perovskites: optically active crystal phase stability to surface engineering," Micromachines, vol. 13, p. 1318, 2022.

W. Wang, Z. Gao, J. Chen, and F. Liu, "Optimizing the substrate pre-heating and post-annealing temperatures for fabricating high-performance carbon-based $CsPbIBr_2$ inorganic perovskite solar cells," Electrochim. Acta, vol. 349, 136354, 2020.

Online ISSN 3007-3197
Print ISSN 3007-3189

M. Raj, S. Patel, and N. Singh, "Recent progress in cesium-based lead-free halide double perovskite materials for photovoltaic applications," Phys. Status Solidi A, vol. 219, 2200425, 2022.

Y. H. Khattak, M. Usman, and A. Rehman, "Advancements in bandgap engineering: bromide-doped cesium lead perovskite thin films," J. Mater. Sci.: Mater. Electron., vol. 19, no. 14, 2024.

M. I. Hossain, T. Ahmed, and R. Alam, "Revealing the full potential of $CsPbIBr_2$ perovskite solar cells: advancements towards enhanced performance," Mater. Horiz., 2024.

D. A. Idosa, J. Kim, and P. Lee, "Cesium lead bromide perovskite nanocrystals synthesized via supersaturated recrystallization at room temperature: comparison of one-step and two-step processes," Nanoscale Adv., 2024.

J. K. Nam, M. S. Jung, S. U. Chai, Y. J. Choi, D. Kim, and J. H. Park, "Resistance switching effect of memory device based on all-inorganic $CsPbBrI_2$ perovskite," PMC, 2021.

Z. Li, Q. Chen, H. Guo, and J. Xu, "Thermodynamically stabilized β-$CsPbI_3$-based perovskite solar cells with efficiencies >18%," Science, vol. 365, no. 6453, pp. 591–595, 2019.

S. B. Jaffri, L. Khan, and P. Ali, "[Ce-Pr-Nd]:$CsPbI_{1.8}Br_{1.2}$: Stability-enhanced light harvester in perovskite solar cells," J. Energy Storage, vol. 67, 107566, 2023.

X. Zhao, L. Zhang, and R. Huang, "Efficient all-inorganic $CsPbIBr_2$ perovskite solar cells with an open voltage over 1.33 V by dual-additive strategy," Surf. Interfaces, vol. 40, 103145, 2023.

L. Scalon, P. Rossi, and F. Moretti, "Tiny spots to light the future: advances in synthesis, properties, and application of perovskite nanocrystals in solar cells," Nanoscale, vol. 15, no. 3, pp. 907–941, 2023.

A. Singh, V. Gupta, and R. Kumar, "Recent trends in $CsPb(Br,I)_3$ mixed-halide perovskites: optoelectronic properties and applications," J. Mater. Chem. C, vol. 11, pp. 12345–12360, 2023.

Song, Z., et al. (2019). "Luminescent perovskites: recent advances in theory and experiments." Inorganic Chemistry Frontiers 6(11): 2969-3011.

Yu, J., et al. (2025). "Double-Pulse Laser Direct Writing-Induced Crystallization and Luminescence Enhancement of Perovskite Nanocrystals for In Situ Patterning." ACS Applied Nano Materials 8(20): 10595-10602.

Zakaria, M. Q., et al. (2025). "Ultrafast Laser Irradiation Enhances Crystallinity and Photoluminescence of Colloidal CsPbBr3 Nanocrystals for High-Performance X-ray Detection." ACS Applied Nano Materials.

Song, Z., et al. (2019). "Luminescent perovskites: recent advances in theory and experiments." Inorganic Chemistry Frontiers 6(11): 2969-3011.

Song, Z., J. Zhao, and Q. Liu, Luminescent perovskites: recent advances in theory and experiments. Inorganic Chemistry Frontiers, 2019. **6**(11): p. 2969-3011.